

In celebration of the 60th birthday of Dr Andrew K. Galwey

THE DEHYDRATION OF COPPER(II) ACETATE MONOHYDRATE

M. C. Ball and L. Portwood

Department of Chemistry, Loughborough University of Technology Loughborough, Leics,
LE11 3TU, UK

Abstract

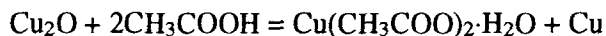
The thermal dehydration of copper(II) acetate hydrate has been studied between 353 and 406 K, over a range of humidities. The dehydration is controlled by nucleation-and-growth kinetics at low temperatures, with an activation energy of $154 \text{ kJ}\cdot\text{mol}^{-1}$, which changes to contracting-disc kinetics at higher temperatures with a lower activation energy of $76 \text{ kJ}\cdot\text{mol}^{-1}$. Frequency factors have also been derived; the value for the high temperature process is low (10^7 s^{-1}) and that for the low temperature step is high (10^{17} s^{-1}). Optical microscopy has been used to clarify the bulk kinetics; there is evidence for a reactive layer at the surface of the decomposing solid.

Keywords: copper(II) acetate monohydrate, dehydration, kinetics, solid state decomposition

Introduction

Bronze disease results when the surface patina on the alloy, consisting of copper(I) oxide and/or chloride, breaks down, and copper(II) salts are formed [1]. The identity of these product salts depends on the conditions (particularly of humidity) and on the patina composition, but generally consist of salts of general formula $\text{Cu}_2(\text{OH})_3\text{X}$ where X is chloride, sulphate or nitrate [2, 3].

Copper(II) acetate has been suggested as possible precursor to bronze disease [4], by the reaction of the patina with acetic acid released from wood shavings (used for storage), followed by oxidation or disproportionation and then partial hydrolysis (to produce the basic acetate and free acetic acid), thus initiating a cycle of corrosion, as follows:





The present work, therefore, aims to study the dehydration of the monohydrate, to find any evidence for the formation of the basic acetate and free acetic acid, using a range of humidities as well as temperature as variables.

The dehydration of copper(II) acetate monohydrate has been studied previously [5, 6]. Contracting-geometry kinetics were observed, but with different values of activation energy depending on whether single crystals or powders were used. Non-integral values of n were observed in the contracting-geometry equations. No evidence was found for the formation of the basic salt.

Experimental

Starting material

Copper(II) acetate monohydrate (Aldrich, 99.9%) was recrystallised from distilled water containing acetic acid, filtered, dried in a desiccator containing silica gel, and stored in a refrigerator. The material consisted mainly of crystals elongated along b_0 , 1–2 mm in length, with an aspect ratio of approximately five.

Mass loss studies

The mass losses at constant temperature were followed using sample masses of $8 \text{ mg} \pm 1 \text{ mg}$, and a Stanton TG-750 thermobalance operating isothermally. A nitrogen flow of $10 \text{ ml} \cdot \text{min}^{-1}$ was passed over the sample. This gas stream was kept at constant humidity, controlled by bubbling the gas through saturated salt solutions at 298 K or over silica gel [7]. The temperature range studied was between 353 and 406 K.

Microscopy

Single crystals of the monohydrate were heated on a normal microscope hot-stage, and the early stages of the decomposition studied by transmission optical microscopy. The stage temperature was monitored by a thermometer inserted close to the centre of the stage, immediately below the sample.

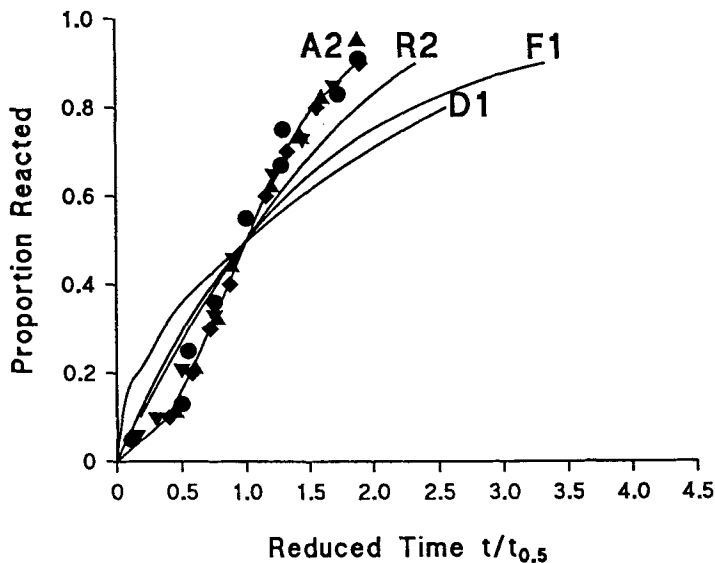


Fig. 1 Reduced-time plot for the low-temperature dehydration of copper(II) acetate monohydrate \blacktriangle 355 K/0%RH \blacktriangledown 355 K/53%RH \blacklozenge 362 K/96%RH \bullet 370 K/53%RH
 A2 = Avrami-Erofeyev equation, $n = 2$, R2 = Contracting-disc equation, F1 = First-order equation, D1 = Parabolic law

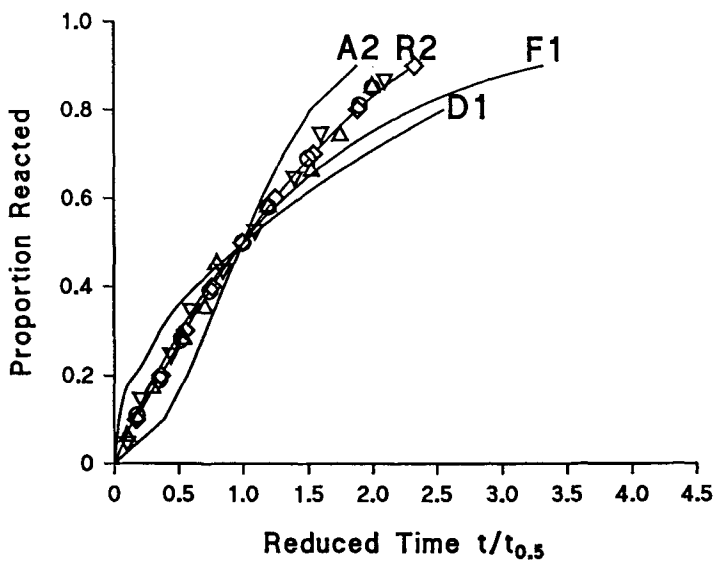


Fig. 2 Reduced-time plot for the high-temperature dehydration of copper(II) acetate monohydrate. \triangle 371 K/0%RH \triangledown 371 K/53%RH \diamond 385 K/96%RH \circ 390 K/0%RH Other symbols as in Fig. 1

Results

Mass losses

Experimental mass losses (9.00%) were those expected for the loss of water only (9.02%). No high values were obtained, nor was any MS evidence obtained for the loss of acetic acid.

Kinetics

The isothermal mass-loss curves were analysed by the method of reduced-time plots, based on the time for 50% reaction [8]. The experimental reduced-time plots were compared with models based on nucleation-and-growth, phase-boundary, or diffusion control of the reaction.

Reaction mechanisms

At temperatures between 371 and 406 K, the best fit between experimental and model reduced-time plots was in terms of the two-dimensional phase boundary equation (contracting disc):

$$(1 - (1 - \alpha)^{1/2}) = kt$$

where α = proportion decomposed.

Figure 1 shows a reduced-time plot for the data gathered in this temperature range.

At lower temperatures, the best fit was with the Avrami-Erofeyev equation with $n = 2$:

$$-\ln(1 - \alpha) = kt^2$$

A reduced-time plot is shown in Fig. 2 for this temperature range. No effect was noted with variation of water-vapour pressure. The derived rate constants have been converted into an Arrhenius plot shown in Fig. 3.

Microscopy

Single crystals were decomposed on a hot stage at two temperatures, corresponding to the nucleation-and-growth and contracting-disc regions (355 and 400 K respectively). Usually, the stage temperature was set to the chosen temperature and was constant before the crystals were placed in position. A few experiments were undertaken in which the stage (with a crystal in position) was

warmed from room temperature to the lower of the two chosen temperatures. Little difference was noted between the two treatments.

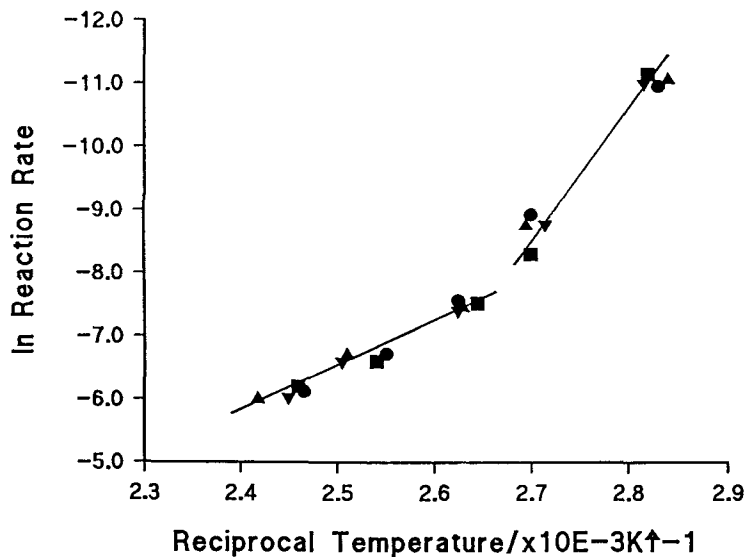


Fig. 3 Arrhenius plot for the dehydration of copper(II) acetate monohydrate. \blacktriangle 0%RH
 \blacktriangledown 4%RH \blacksquare 53%RH \blacklozenge 96%RH

Low temperature decomposition

The starting material (Fig. 4) showed reasonably flat faces with some smaller pieces of material attached plus some larger defects.

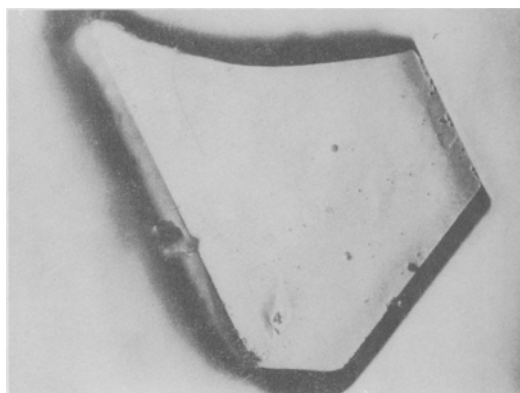


Fig. 4 298 K. Magnification $\times 250$

On heating at 355 K, the whole surface became paler and some puckering became visible. Multiple short cracks appeared after a few minutes, forming star-shaped nuclei (Fig. 5). With longer times, cracks appeared which linked the initial nuclei, and some lightening of parts of the surface adjacent to the cracks became obvious (Fig. 6). It was clear that these lighter parts were caused by lifting of parts of a surface layer. The density of the nuclei varied with the crystal face (Figs 7 and 8).

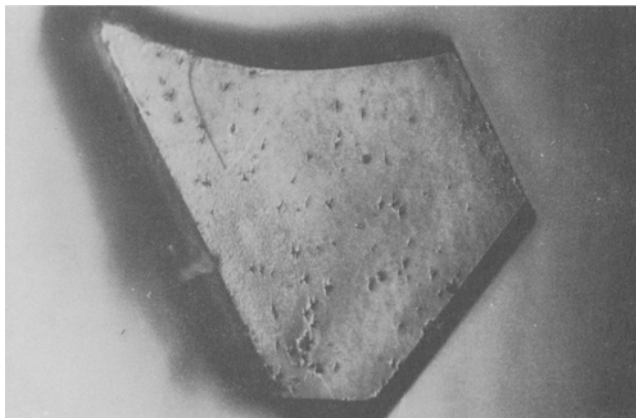


Fig. 5 355 K. Magnification $\times 250$

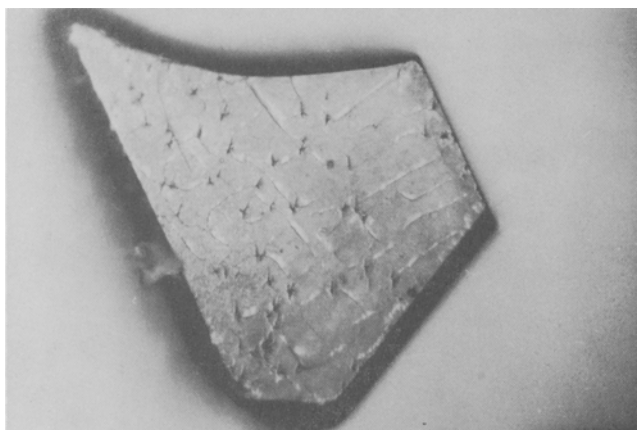


Fig. 6 355 K. Magnification $\times 250$

High temperature decomposition

High temperature decomposition gave no sign of star-shaped nuclei, but did produce very large cracks, many of which were at approximately right angles to the long axis of the crystal (Fig. 9).

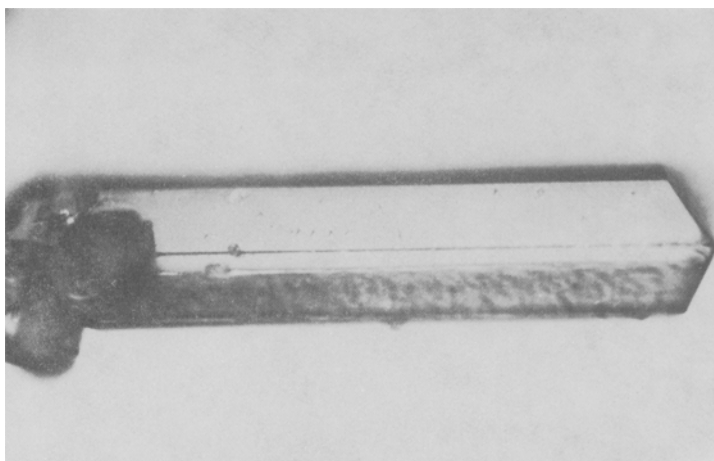


Fig. 7 355 K. Magnification $\times 250$. Upper face in focus

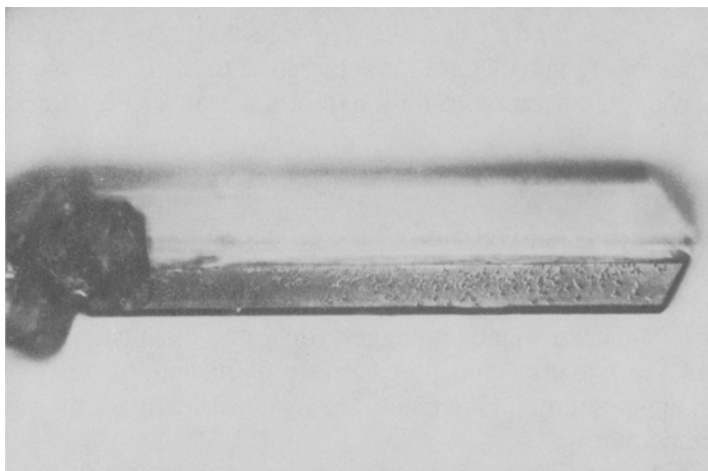


Fig. 8 355 K Magnification $\times 250$. Lower face in focus

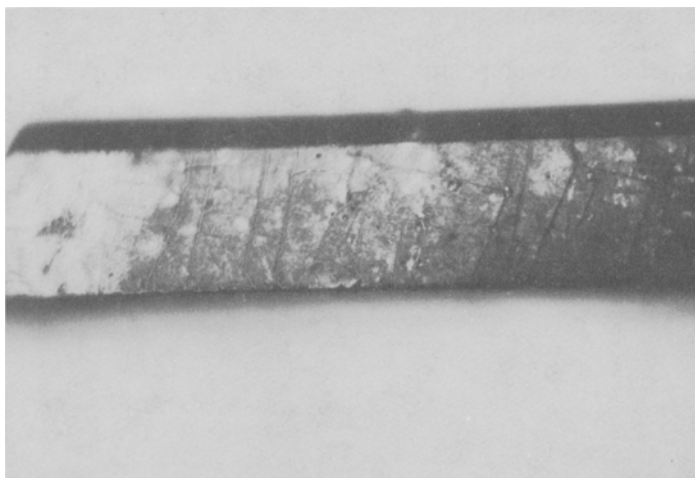


Fig. 9 400 K. Magnification $\times 250$

Discussion

Mass losses

All of the runs gave mass losses very close to the theoretical value for dehydration. No additional mass losses which might indicate the release of acetic acid and the formation of a basic salt were detected. Mass spectroscopy confirmed the lack of organic material. It is therefore unlikely that the basic salt is produced at room temperature to form part of the bronze corrosion cycle.

Reaction mechanisms

A normal kinetic interpretation of the reduced-time plots shown in Fig. 1 would indicate that the Avrami-Erofeyev equation describes the low-temperature dehydration, and the contracting-disc equation describes the high-temperature behaviour. These together suggest that two-dimensional geometry is important in the reaction, and that the rate of nucleus formation increases greatly with temperature, giving rise to the rapid formation of the surface layer at higher temperatures.

The straight-forward derivation of Arrhenius parameters from Fig. 4 gives activation energies of 76 and 154 $\text{kJ}\cdot\text{mol}^{-1}$ for the high and low temperature stage respectively and values of $1.6\times 10^7 \text{ s}^{-1}$ and $8.5\times 10^{17} \text{ s}^{-1}$ respectively, for the high and low temperature frequency factors. These values would suggest

that both the nucleation and the growth stages in the dehydration reaction have about the same activation energies, viz., 75 kJ mol^{-1} , and that the transition state for the low temperature step has more degrees of freedom than the higher temperature one. This latter point would suggest that the transition state does not involve any surface states [9].

The Arrhenius parameters for the two mechanisms may indicate the operation of a compensation effect [10, 11] in which high activation energies are compensated for, in rate terms, by high frequency factors, according to the relationship:

$$\log A = B + eE$$

where A and E are the frequency factor and the activation energy, and B and e are constants, the compensation parameters. The present values are too few in number to be given much weight, but the compensation parameters determined from them ($B = -3$, $e = 0.125$), lie reasonably close to those derived for a range of decomposition reactions ($B = -5.02$, $e = 0.067$) [12] and are very different from those derived from genuine catalytic reactions [11].

Microscopy

The micrographs indicate, despite the above kinetic analysis, that the dehydration is rather more complex, and that the formation of nuclei is not the same as that typically shown in many dehydration reactions [13], in that cracks appear, rather than outgrowths of dehydrated product. However, these cracks behaved as normal 'nuclei' in that they could be described as two-dimensional, and the number of them did not vary with time (i.e. $dN/dt = 0$). In the normal Avrami-Erofeyev description, $n = 2 = \gamma + \delta$; $\gamma = 2$, and $\delta = 0$.

There is some similarity to the group of dehydrations studied by Galwey and his co-workers, which indicate the formation of a surface layer, with the behaviour of this layer controlling the kinetics [14]. The nuclei formed in the present dehydration are much simpler than some of those observed previously [13, 14], and can easily be related to cracking of the surface layer under tensile stress brought about by shrinkage. This shrinkage produces star-shaped 'nuclei' which apparently control the kinetics. Such stress-cracking frequently produces ordered patterns [15]. This stressed layer can lift off the surface during the later stages of reaction. Such behaviour has also been noted during drying of particulate solids [15].

The decomposition at higher temperatures shows no nuclei, only a fairly rough surface with large cracks. This can be interpreted as indicating that the loss of water from the surface, and hence the stress build-up, is so rapid that it

can only be released by massive breakdown, with the formation of very large cracks.

Comparison with previous work

The previous work on this dehydration [5, 6] suggested that different processes occurred depending on the use of single crystals or powdered material. Both dehydrations followed contracting-geometry kinetics, but the activation energy varied from $120 \text{ kJ}\cdot\text{mol}^{-1}$ for single crystals to $86 \text{ kJ}\cdot\text{mol}^{-1}$ for crushed powders. These numerical values are not very different from those obtained in the present work; the difference in rate-controlling process cannot be explained.

References

- 1 Z. Goffer, *Archeological Chemistry*, Wiley, 1980, p. 260.
- 2 A. F. Wells, *Structural Inorganic Chemistry*, 3rd Edition, O.U.P., 1962, p. 392.
- 3 H. R. Oswald and W. Feitnecht, *Helv. Chim. Acta*, 44 (1961) 272. W. Feitnecht, 'Essays in Coordination Chemistry', Ed. W. Schneider, G. Anderegg and R. Gut, Birkhauser Verlag, Basel, 1964, p. 84.
- 4 R. Walker, *J. Chem. Ed.*, 57 (1980) 277.
- 5 N. Koga and H. Tanaka, *Solid State Ionics*, 44 (1990) 1.
- 6 H. Tanaka and N. Koga, *Thermochim. Acta*, 173 (1990) 53.
- 7 J. F. Young, *J. App. Chem.*, 17 (1967) 24.
- 8 J. H. Sharp, G. W. Brindley and B. N. N. Achar, *J. Amer. Ceram. Soc.*, 49 (1966) 379.
- 9 H. F. Cordes, *J. Phys. Chem.*, 72 (1968) 2185.
- 10 A. K. Galwey, *Adv. Cat.*, 26 (1977) 247.
- 11 A. K. Galwey and M. E. Brown, *J. Catal.*, 60 (1979) 335.
- 12 M. C. Ball and M. J. Casson, *J. Thermal Anal.*, 28 (1983) 371.
- 13 W. E. Garner (Ed.), *Chemistry of the Solid State*, Butterworth, London, 1955, Ch. 8.
- 14 A. K. Galwey, R. Spinicci and G. G. T. Guarini, *Proc. Roy. Soc. London*, A378 (1981) 477.
- 15 J. Walker, *Scientific American*, 255 (1986) 178.

Zusammenfassung — Im Intervall 353-406 K und bei verschiedener Feuchte wurde die thermische Dehydratation von Kupfer(II)-acetat-Hydrat untersucht. Bei niedrigen Temperaturen wird die Dehydratation durch eine Kernbildungs- und Kernwachstumskinetik mit einer Aktivierungsenergie von 154 kJ/mol kontrolliert, was bei höheren Temperaturen in eine Kinetik kontraktierender Scheiben mit einer niedrigeren Aktivierungsenergie von 76 kJ/mol übergeht. Die Frequenzfaktoren wurden ebenfalls ermittelt; der Wert für den Prozeß bei höherer Temperatur ist niedrig (10^7 s^{-1}) und der für den Schritt bei niedrigerer Temperatur groß (10^{17} s^{-1}). Zur Klärung der Volumen-Kinetik wurde optische Mikroskopie angewendet; es gibt Beweise für eine reaktive Schicht an der Oberfläche des sich zersetzenden Feststoffes.